IMPULSIVE MOTION OF VISCOUS AXISYMMETRIC LIQUID BRIDGES*

J. Meseguer[1], J.M. Perales[1] and N.A. Bezdenejnykh[2]

1) Lamf-μg, Laboratorio de Aerodinámica, E.T.S.I. Aeronáuticos, Universidad Politécnica, 28040 Madrid, Spain

2) Institut Mekhaniki Sploshnykh Sred, Permski Nauchnyi Centr (Uralskoe Otdelenie AN SSSR), 614061 Perm, USSR.

ABSTRACT

This paper deals with the dynamics of isothermal, axisymmetric, viscous liquid columns held by capillary forces between two circular, concentric, solid disks. The transient response of the bridge to an excitation consisting of a small change in the value of the acceleration acting along its axis has been considered. To compare existing theoretical results with experimental ones a number of experiments have been performed; in these experiments, a small liquid bridge with its axis placed vertically was suddenly displaced downwards for a small distance and the response of the interface recorded, the agreement between theoretical and experimental results (damping time constant) being good enough.

Keywords: *Liquid bridge, Microgravity, g-jitter.*

1. INTRODUCTION

The liquid bridge configuration considered here consists, as sketched in Figure 1, of an isothermal, axisymmetric mass of liquid held by surface tension forces between two parallel, coaxial, circular solid disks. Such a fluid configuration can be uniquely identified by the following set of dimensionless parameters: the ratio of the radius of the smaller disk, R_1, to the radius of the larger one R_2, $K=R_1/R_2$; the slenderness, $\Lambda=L/2R_o$, where $R_o=(R_1+R_2)/2$ and L is the distance between both disks; the dimensionless volume of liquid, $V=V/R_o^3$, V being the physical volume; the Bond number, $B=\rho g R_o^2/\sigma$; and the capillary number, $C=\nu(\rho/\sigma R_o)^{1/2}$, where ρ is the liquid density, g the axial acceleration, σ the surface tension and ν the kinematic viscosity.

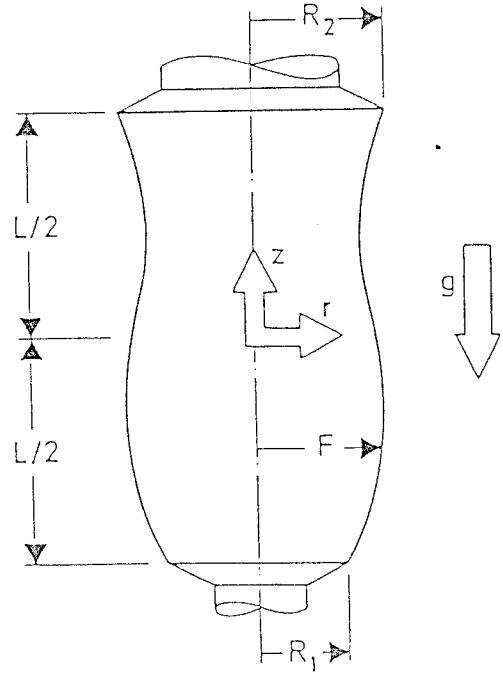

Figure 1. Geometry and coordinate system for the liquid bridge problem.

* Dedicated to the memory of Prof. I. da Riva

Most of the published studies related to the liquid bridge response to forcing perturbations are concerned with harmonic perturbations (Refs. 1 to 5). Non-harmonic perturbations have been considered in Ref. 6, where a one-dimensional inviscid slice model was used to analyze the liquid injection or removal in the liquid bridge and in Ref. 7, where the same problem here considered is analytically solved by using a one-dimensional Cosserat model, including viscosity effects, although in that case the analysis is restricted to cylindrical liquid bridges ($V=V_c=2\pi\Lambda$) between equal disks ($K=1$) and in gravitationless conditions ($B=0$) (in this case the interface at rest is a cylinder).

A linear theoretical model of the dynamic response of viscous axisymmetric liquid bridges due to small changes in the value of the axial acceleration acting on the liquid has been developed (Ref. 8) by using the Cosserat's one-dimensional model for continuum media. This model has been used for capillary jet problems and for liquid bridge problems, and has proved to give satisfactory results, when compared with 3-D models results, provided that the slenderness of the liquid bridge is large enough ($\Lambda > 1$).

In order to check the above theoretical predictions, the transient response of liquid bridges subjected to a small perturbation in the axial acceleration has been measured. Experiments have been carried out by working with very small liquid bridges ($R_o=0.5 \times 10^{-3}$ m) and using distilled water as working fluid. The liquid bridge, initially at rest, is suddenly displaced vertically a distance of the order of R_o and the subsequent evolution recorded, so that the damping time constant of the evolution until the final equilibrium state is measured. A number of experiments have been performed, varying either the volume of liquid or the distance between disks, experimental results showing the same trends as theoretical predictions.

2. THEORETICAL RESULTS

Before pursuing further it would be convenient to point out some characteristics of the liquid bridge response, stated in Ref. 7 for cylindrical liquid bridges between equal disks (obviously the behaviour is qualitatively the same no matter the values of V, K, and B are, provided the liquid bridge configuration is stable). In the following we will denote as $h_n=\gamma_n+i\omega_n$ the roots of the secular equation deduced by the analysis of the problem in the Laplace domain. For a given liquid bridge configuration, that is, once Λ, K, B and V are fixed, all the roots are imaginary ($\gamma_n=0$) if $C=0$, and consequently the liquid bridge response will be oscillatory, without damping, as one could expect from an inviscid movement, and all the oscillation modes will be present in the liquid bridge response. As C increases, the value of γ_n becomes more and more negative, whereas the absolute value of ω_n decreases. That means that all oscillation modes are damped, their oscillation frequencies being smaller as C grows. For each oscillation mode there is a critical value $C=C_n^*$ beyond which the associated movement is only damped, without oscillation ($\omega_n=0$).

Concerning the importance of the different oscillation modes in the liquid bridge dynamics it must be pointed out that the only significative oscillation mode is the first one by two reasons. The first one concerns the amplitude of the different oscillation modes, much larger in the first oscillation mode than in the following ones and the second is that, in the case of damped oscillations, the absolute value of γ_n increases as the index of the oscillation mode, n, grows; therefore, all oscillation modes are damped much quicker than the first one (oscillation modes different from the first one are only important for short times when all of them appear to fulfill the initial conditions).

The same qualitative behaviour can be observed when a variation of the Bond number, the disk diameter ratio or the volume is considered. Even more, for a given value of C the resonance frequency, ω_1, decreases and the absolute value of damping factor, γ_1, increases as the liquid bridge configuration approaches the corresponding stability limit; close enough of the stability limit there is a region in which $\omega_1=0$ and the absolute value of γ_1 decreases. The damping factor becomes zero at the stability limit and it is greater than zero for unstable liquid bridge configurations (Refs. 7-9)

The dependence on the dimensionless parameter of viscosity, C, of the real and imaginary parts of the roots corresponding the first oscillation mode, γ_1 and ω_1, are shown in Figure 2, the main characteristic to be pointed out from this plot being that the damping factor γ_1 varies almost linearly with C no matter the values of the remaining liquid bridge parameters are. This linear dependence of γ_1 on C is of great help when theoretical results are compared with experimental ones because it allows the comparison of both types of results independently of the value of surface tension, which is difficult to measure.

3. EXPERIMENTAL RESULTS

The experimental set-up, as sketched in Figure 3 (not to scale) consists of a liquid-bridge rig (although in Figure 3 only the liquid bridge is shown (1)), background illumination (2), a microscope (3) to which a CCD

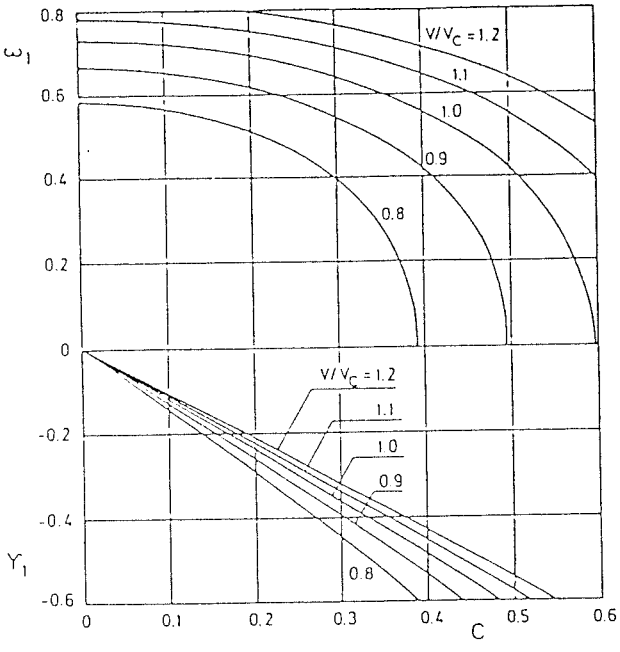

Figure 2. Variation with the dimensionless viscosity parameter, C, of the resonance frequency, ω_1, and damping factor, γ_1, corresponding to the first oscillation mode. Numbers indicate the value of V/V_C. These results correspond to liquid bridges with Λ=2, K=1 and B=0 (from Ref. 8).

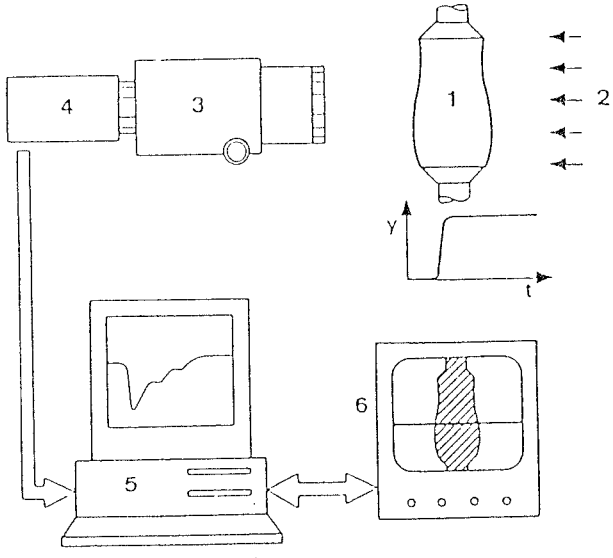

Figure 3. Experimental set-up. 1) Liquid bridge; 2) illumination; 3) microscope; 4) CCD camera; 5) computer; 6) TV monitor.

camera (4) is connected, a desktop computer (including data acquisition and image processing systems (5)) and a TV monitor (6). The liquid-bridge rig (LB rig) consists of a closed test chamber having two opposite lateral sides made of glass to allow visualization. The liquid bridge is formed inside the test chamber between two coaxial solid disks made of Perspex (10^{-3} m in diameter) their common axis being vertical during experiments. The bottom disk is fixed to the rig frame, whereas the upper one can be displaced upwards and downwards as well as rotated. During experiments a small volume of water was poured at the bottom of the test chamber to keep the air inside the test chamber saturated, thus avoiding the evaporation of water (which was used as working liquid) from the liquid bridge once formed, which could cause the variation with time of the liquid bridge volume. The bottom disk incorporates the filling duct (which ends at a hole, less than 0.5×10^{-3} m in diameter, at the centre of the bottom disk). The liquid bridge is formed by injecting some amount of water from an external syringe; once a small drop of liquid is formed on the bottom disk, the upper one is displaced downwards until it is contacted and wetted by the water drop, and a short liquid bridge spanning between both disks results. From now on the distance between disks is slowly increased, injecting water at the same time, until the desired slenderness and volume of liquid are reached.

The whole LB rig is mounted on an electric shaker which is driven by an electric-signal generator. The shaker was adjusted in such a way that its axis moves upwards a distance of 0.3×10^{-3} m, as sketched in the insert in Figure 3 and in Figure 4, when required.

For illumination, to avoid the excessive heating of the LB rig, a cold source of light was used: a lamp placed some distance apart of the rig, the light being conducted through an optic–fibre cable. Using the appropriate background illumination the liquid bridge appears in the TV screen as a black shadow with a well defined contour on a white background. With the capabilities of the image processing system used it is possible to get either the whole contour, which is used to calculate the slenderness of the liquid bridge as well as its volume (it takes about 1 s to determine Λ and V), or to get the time evolution, at a rate of 25 frames/second, of up to three different sections of the liquid bridge.

The experimental procedure was as follows: once the liquid bridge is formed and the slenderness and volume determined as indicated above, the second choice for the image processor (variation with time of the liquid bridge contour at some prefixed section) is selected and a starting pulse is sent to the shaker (averaged nominal profiles of the displacement, velocity and acceleration experienced by the whole liquid bridge are shown in Figure 4). Because of the impulsive acceleration acting on the liquid bridge its interface distorts and a damped oscillation with the corresponding natural frequency starts. Once the liquid bridge is at rest again, and the

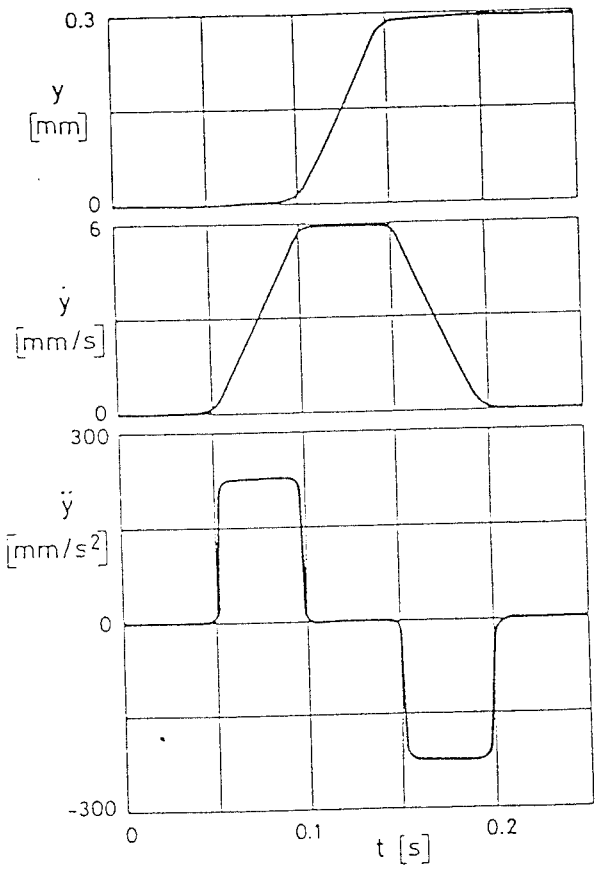

Figure 4. Typical variation with time, t, of the axial displacement, y, velocity, $\dot{y}$, and acceleration, $\ddot{y}$, of the LB rig during experiments.

shaker axis returned to its initial position, some amount of liquid is injected (or removed) into the liquid bridge to get a new volume of liquid (provided the liquid bridge is still formed, otherwise it would be necessary forming a new liquid bridge as explained above) and the next experiment can start.

Unfortunately, this experimental set-up is only appropriate to measure damping time constant but not natural frequencies, the reason being that the scanning rate in normal video signal is 25 frames/second whereas natural frequencies of the tested configuration are higher than 25 Hz (Ref. 1). Typical evolutions of different liquid bridge configurations (the variation with time, t, of the radius of the liquid bridge, $f=F(t) - F(0)$, at the measurement section) are shown in Figure 5. Note that in these plots the final value of f is not zero; this is because of the perturbation imposed (a quick axial displacement of the liquid bridge): the liquid bridge moves in respect to the scanning line in the TV screen so that the time variation of the interface radius is measured at a different section of the initial one. For each experiment a time-exponential function has been fitted to experimental data and the damping factor obtained.

A problem arising when comparing experimental and theoretical results is that surface tension appears in most of the parameters needed for data reduction, namely: characteristic time, $t_c=(\rho R_o^3/\sigma)^{1/2}$; viscosity parameter, $C=\nu(\rho/\sigma R_o)^{1/2}$ and Bond number, $B=\rho g R_o^2/\sigma$. Surface tension of water can vary almost an order of magnitude

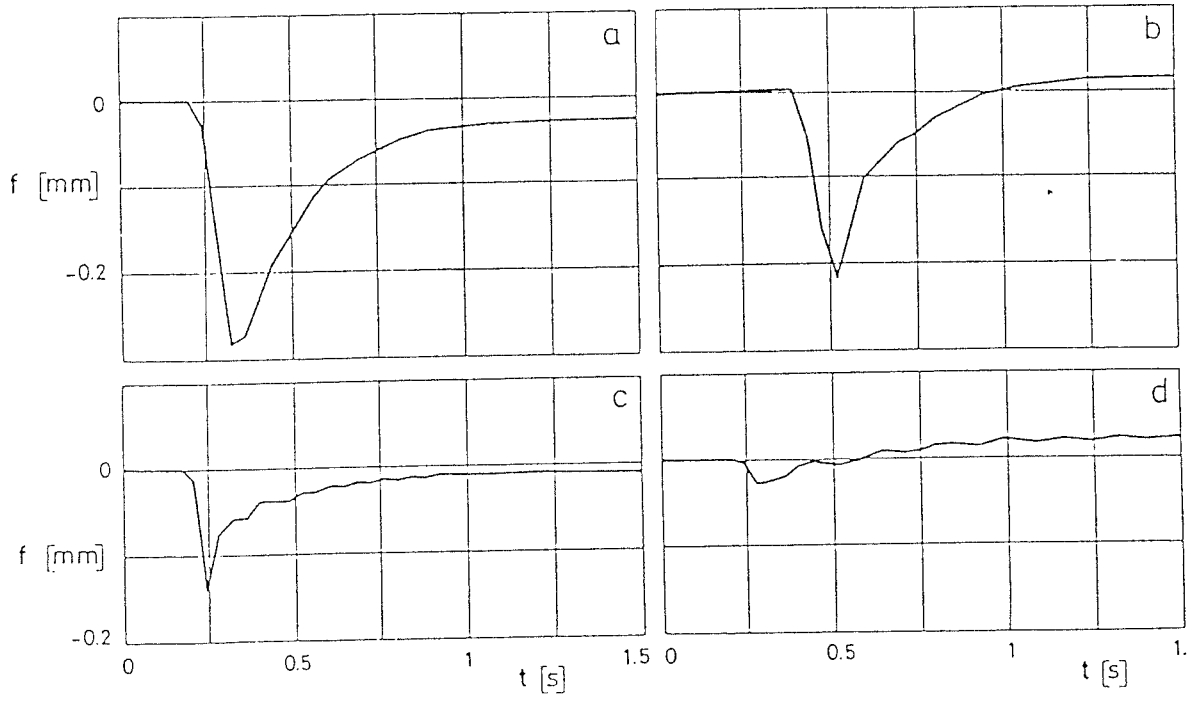

Figure 5. Variation with time, t, of the radius of the liquid bridge interface at the measurement section, $f=F(t) - F(0)$. a) $\Lambda = 2.04$, $V/V_C = 0.88$; b) $\Lambda = 2.04$, $V/V_C = 1.10$; c) $\Lambda = 2.49$, $V/V_C = 0.98$; d) $\Lambda = 2.49$, $V/V_C = 1.35$, where $V_C=2\pi\Lambda$.

depending on the degree of surface contamination, assuming a variation from 0.06 $N.m^{-1}$ to, let say, 0.02 $N.m^{-1}$ (in other experiments using water as working fluid performed with the same set-up the value σ=0.06 $N.m^{-1}$ was measured, Ref. 10) and taking into account the nominal values of the remaining physical parameters of the experiments (R_o=5 x 10^{-4} m, ρ=10^3 $kg.m^{-3}$, ν=1.08 x 10^{-6} $m^2.s^{-1}$, g=9.81 $m.s^{-2}$), one gets that Bond number can range between 0.04 and 0.12, that viscosity parameter would be between 0.006 and 0.010 and that the value of characteristic time is between 1.4 x 10^{-3} s and 2.5 x 10^{-3} s.

The damping factor depends on Λ, K, B, V and C. Once the four first parameters are fixed, the dependence on C is linear provided C is small enough (as shown in Figure 2). Therefore, the dimensionless damping factor can be expressed as $\gamma_1=mC$ where $m=m(\Lambda,K,B,V)$, so that the physical damping factor, $\bar{\gamma}_1$ will be

$$\bar{\gamma}_1 = \frac{\gamma_1}{t_c} = \frac{mC}{t_c} = \frac{mV}{R_o^2} = 4.3m(\Lambda,K,B,V) \quad \left[s^{-1}\right]$$

In the experiments performed both disks were equal in diameter (K=1) and the slenderness and the volume of liquid were measured with high accuracy as explained above. Nevertheless, there is some uncertainty concerning the value of Bond number due to the uncertainty in the value of the surface tension. The different experiments performed are summarized in Figure 6. In this plot each one of the experiments is represented by a circle in the Λ–V stability diagram (K=1). Also in this plot the stability-limit curves corresponding to B=0, 0.05 and 0.1 are shown. Obviously, since all the liquid bridge configurations tested were stable, this plot gives an upper limit for the value of Bond number which corresponds to a high value of surface tension (σ ~ 0.05 $N.m^{-1}$).

Experimental results (damping factor versus reduced liquid bridge volume, V/V_c, where $V_c=2\pi\Lambda$) are compared with theoretical ones in Figure 7, for liquid bridges with Λ=2.04, and in Figure 8 (for the case Λ=2.49). In these plots theoretical curves corresponding to different values of Bond number have been represented. Note that experimental data shows the same trends as theoretical predictions, although they are too scattered.

Acknowledgements

This work has been performed during a stay of Dr. Bezdenejnykh at Lamf-µg (Madrid) sponsored by the European Space Agency (ESA) and the Universidad Politécnica de Madrid. This work has been supported also by the Comisión Interministerial de Ciencia y Tecnología (CICYT), Project No. ESP88-0359.

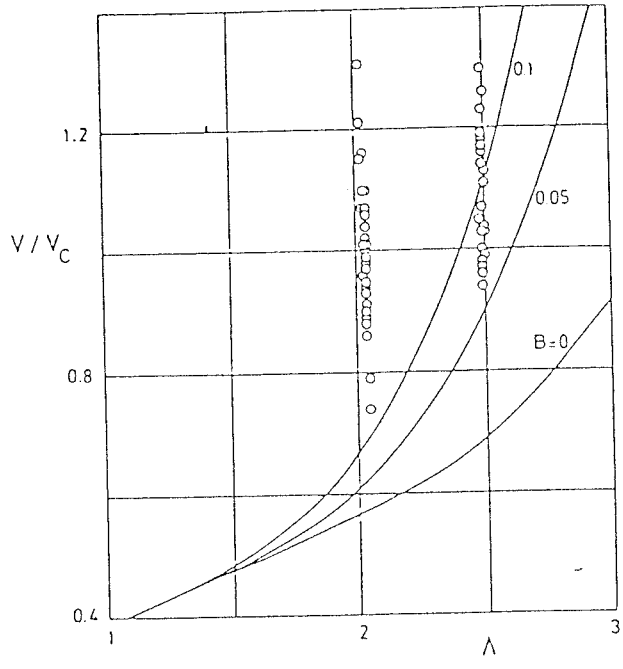

Figure 6. Minimum volume stability limit for different Bond numbers (0, 0.05 and 0.1). Circles show conditions where damping time constant has been measured.

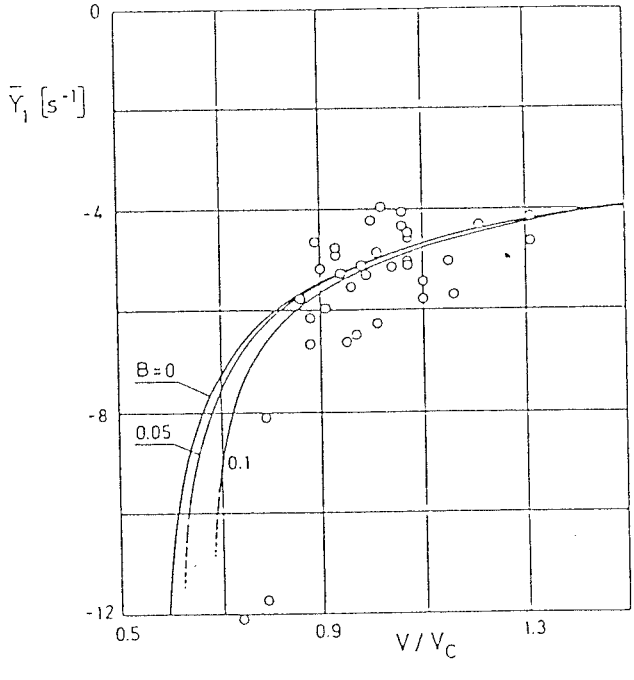

Figure 7. Damping factor, $\bar{\gamma}_1$, as a function of reduced volume, V/V_c for liquid bridges with slenderness Λ = 2.04. Circles indicate experimental results whereas solid lines show the theoretical ones corresponding to different values of Bond number.

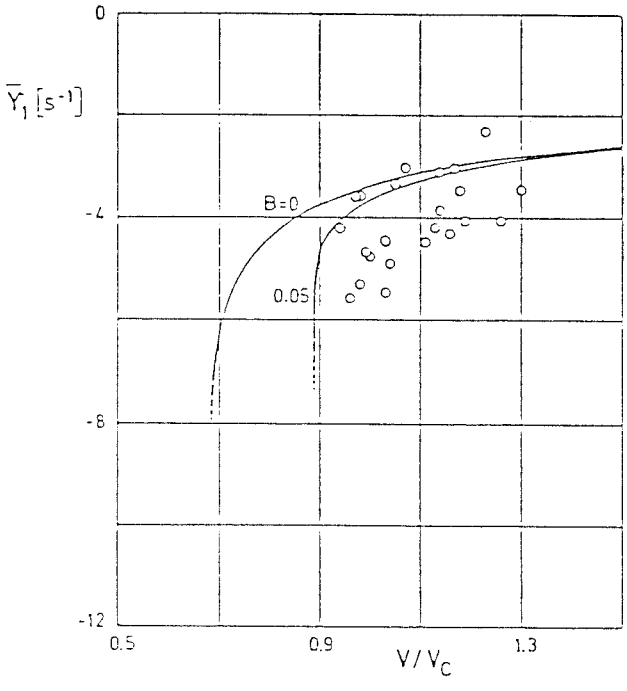

Figure 8. Damping factor, $\bar{\gamma}_1$, as a function of reduced volume, V/V_c for liquid bridges with slenderness $\Lambda = 2.49$. Circles indicate experimental results whereas solid lines show the theoretical ones corresponding to different values of Bond number.

REFERENCES

1.- J. Meseguer, Axisymmetric Long Liquid Bridges in a Time-Dependent Microgravity Field, *Appl. Microgravity Technol.* 1, 136 (1988).

2.- J. Meseguer, A. Sanz and J.M. Perales, Axisymmetric Long Liquid Bridges Stability and Resonances, *Appl. Microgravity Technol.* 2, 186 (1990).

3.- Y. Zhang and J.I.D. Alexander, Sensitivity of Liquid Bridges Subject to Axial Residual Acceleration, *Phys. Fluids A* 2, 1966 (1990).

4.- J.M. Perales, Dinámica de Puentes Líquidos, *Tesis Doctoral*, Universidad Politécnica de Madrid (1990).

5.- J.A. Nicolás, Frequency Response of Axisymmetric Liquid Bridges to an Oscillatory Microgravity Field, *Microgravity Sci. Technol.*, in press.

6.- J. Meseguer and A. Sanz, One-Dimensional Linear Analysis of the Liquid Injection or Removal in a Liquid Bridge, *Acta Astronautica* 15, 573 (1987).

7.- J. Meseguer and J.M. Perales, A Linear Analysis of g-Jitter Effects on Viscous Cylindrical Liquid Bridges, *Phys. Fluids A*, in press.

8.- J. Meseguer, J.M. Perales and N.A. Bezdenejnykh, A Theoretical Approach to Impulsive motion of Viscous Liquid Bridges, *Microgravity Quarterly*, submitted.

9.- J. Meseguer, The Breaking of Axisymmetric Slender Liquid Bridges, *J. Fluid Mech.* 130, 123 (1983).

10.- N.A. Bezdenejnykh and J. Meseguer, Stability Limits of Minimum Volume and Breaking of Axisymmetric Liquid Bridges between Unequal Disks, *Microgravity Sci. Technol.*, in press.